Biotechnology Journal

Supporting Information for DOI 10.1002/biot.201200174

Nanoscale structure of type I collagen fibrils: Quantitative measurement of D-spacing

Blake Erickson, Ming Fang, Joseph M. Wallace, Bradford G. Orr, Clifford M. Les and Mark M. Banaszak Holl

Supporting Information

Nanoscale Structure of Type I Collagen Fibrils: Quantitative Measurement of D-Spacing

Blake Erickson, [1,2#] *Ming Fang,* [2,3#] *Joseph M. Wallace,* [7,*], *Bradford G. Orr,* [2,4,5,*] *Clifford M. Les,* [6] *Mark M. Banaszak Holl*[1,2,3,4,*]

[1]The University of Michigan Program in Biophysics, [2]Michigan Nanotechnology Institute for Medicine and Biological Sciences, [3]Department of Chemistry, [4]Program in Applied Physics, [5]Department of Physics, Ann Arbor, MI 48109

[6]Bone and Joint Center, Henry Ford Hospital, Detroit, MI 48202

[7]Biomedical Engineering, Indiana University- Purdue University, Indianapolis, 723 West Michigan Street, SL 220 Indianapolis, IN 46202-5132

Corresponding Author:

Dr. Mark M. Banaszak Holl

Department of Chemistry

University of Michigan

930 N. University Ave.

Ann Arbor, MI 48109-1055

Telephone: (734) 763-2283 Fax: (734) 763-2283

E-mail: mbanasza@umich.edu

# These authors contributed equally to this manuscript.

Supporting Figure S1: SEM Characterization of the Calibration Standards. Panel a–c are SEM images of 100 nm, 1 µm and 10 µm calibration standards. Listed in the table are the measurements of pitch sizes from the SEM images. The absolute error of the three calibration standards were less than 1.5 %.

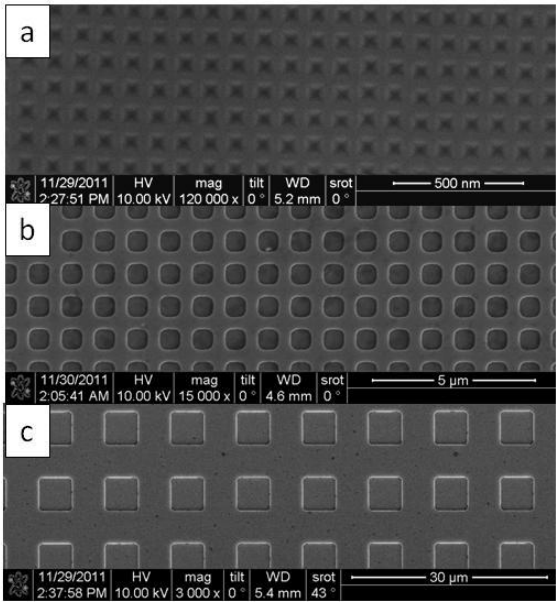

Image	Calibration Standard	X-Pitch Size (µm)	Y-Pitch Size (µm)
a	NANOSENSORS-100 nm	0.1014	0.1009
b	DI-1 µm	1.006	1.010
c	ASYLUM-10 µm	10.12	10.15

SUPPORTING DISCUSSION #1: Example of error calculation from single collagen fibril measurement

Assume the following conditions based on experimental data:

A 3500 nm x 3500 nm image; 512 x 512 pixels; a collagen fibril with a spacing of 67.0 nm and 9 repeats units to measure.

The pixel pitch is therefore 6.8 nm (3500 nm / 512 pixels), which is sampling at 1.50×10^{-1} nm^{-1}. The hypothetical fibril is 603 nm long (88 pixels). The minimum resolvable wavevector is 8.30×10^{-4} nm^{-1}. The reciprocal spacing of the 67.0 nm D-Period spaced fibril is 1.50×10^{-2} nm^{-1}. Dividing the true reciprocal spacing by the wavevector spacing indicates that this spacing will fall into the 18^{th} bin. In this example case, the true peak lies somewhere between 17.5 bins (1.45×10^{-2} nm^{-1} or 68.8 nm) and 18.5 bins (1.54×10^{-2} nm^{-1} or 65.0 nm). With certainty, the spacing is 66.8 nm ± 1.9 nm (28% of a single pixel).

In practice, resolution is higher than this calculation indicates given the signal to noise in the observed peaks. In Figure 1, the observed harmonics have Full Widths at Half Maximum (FWHM) on the order of 2 frequency units. For a Gaussian distribution, the FWHM is defined as $2*(2*\ln 2)^{1/2}*\sigma$ ($\sim 2.35\sigma$), where σ is the standard deviation of the distribution. In Figure 1, σ is ~0.85 bins. The ability to determine the center of a well-resolved Gaussian is easily within 1/4 of σ, or ~ 0.2 bins in Figure 1. Returning to the example above, the peak center would lie between 17.8 and 18.2 bins, corresponding to 67.6 nm and 66.1 nm respectively. It is reasonable to state that the fibril has a D-periodic spacing of 66.8 nm ± 0.8 nm (12% of a single pixel). Further refinements could be made to this error with peak fitting; but, accuracy to a tenth of a nanometer by selecting the peak maximum is sufficient.

Supporting Figure S2: Model Collagen Fibril and Associate Fast Fourier Transform. Panel a shows the construction of the first seven repeat units of a model collagen fibril. The fibril is the summation of multiple Gaussian curves with 65.9 ± 1.0 nm spacing, sampled every 5.0 nm. The width of each Gaussian is 15.0 nm. A constant DC offset has been applied to the amplitude of the fibril. All parameters in the model fibril were experimentally determined from representative AFM scans of Type I collagen fibrils. The 1D FFT shows expected peaks corresponding to the D-periodic spacing, along with short wavelength components. A fit of the data to a function of the form $\gamma e^{\left(\frac{-(f-f_c)^2}{2\sigma^2}\right)}$ is shown in red. In this equation, γ is an amplitude-scaling factor, f is the frequency, f_c is the D-periodic spacing and σ is the associated uncertainty of the D-periodic spacing. The fit to the DC component is shown in blue.

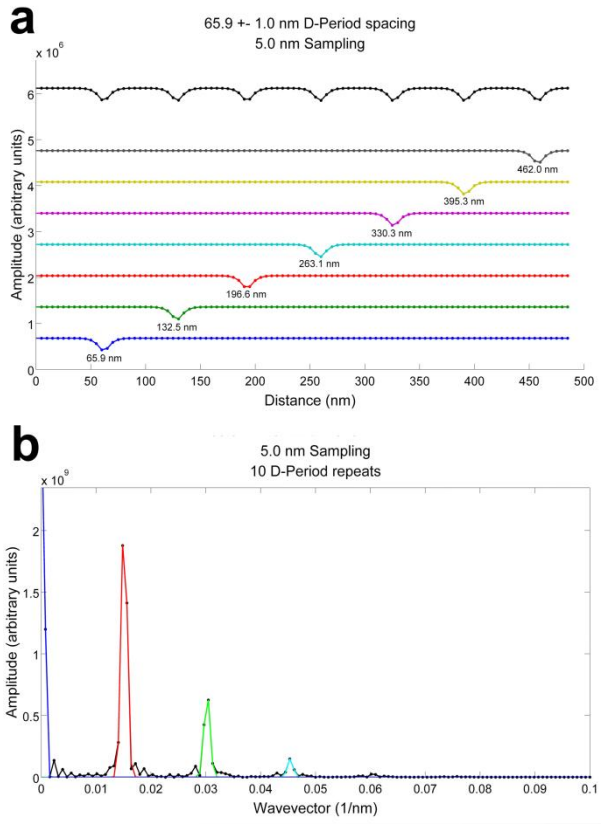

Supporting Table S1: Table of D-Periodic Spacings: This table shows the results of 2D-FFT measurements from multiple Type I collagen fibrils in Sham operated and OVX bone. The D-Periodic spacing for each fibril was computed using a maximum of 21 D-Periods. The mean and standard deviation of the D-Period Spacing of each fibril is shown. The mean of the standard deviations was computed to determine the upper and lower bounds on the D-Period uncertainty. The calculated uncertainty ranges from 0.7 nm for OVX to 0.8 nm for Sham fibrils.

	Sham		OVX	
Fibril	Mean (nm)	Standard Deviation (nm)	Mean (nm)	Standard Deviation (nm)
1	71.3	1.2	59.5	0.4
2	69.5	1.1	59.3	0.9
3	67.6	1.2	63.1	0.6
4	68.0	0.3	61.8	0.7
5	66.4	0.6	61.7	1.0
6	66.1	0.6	65.3	0.9
7	70.2	0.2	65.5	0.5
8	72.2	1.0	65.9	1.0
9	72.2	0.7	61.4	0.5
10	68.9	1.0	61.9	0.7
Mean	69.3	0.8	62.6	0.7
Standard Deviation	2.2	0.4	2.5	0.2

Supporting Figure S3: D-Period Uncertainty Calculation. This figure shows the D-period uncertainty as a function of the number of D-Period repeat units (sample length), and the variability within the spacing used to create a given model fibril. The uncertainty is expected to scale with the number of repeats as 1/x because of finite sampling.[1] An additional component is expected due to the contributions from the inherent variability within a particular fibril. Each data set has therefore been fit to a function of the form $\frac{A}{x} + B$. Both panels show fibrils computed with a range of pixel lengths. A pixel length of 1.0 nm represents an image sampled more than can be achieved experimentally on a real fibril, while lengths of 3.0, 5.0 and 7.0 nm are more experimentally realistic values. (A 3500 nm square image with 512 pixels has a pixel length of 6.8 nm) In both panels, each line is a different pixel density (representing experimental conditions). Panel a shows a fibril with perfect D-period spacing (i.e. no variability in spacing). The B term in all fits approaches 0.0 nm. The lower panel shows the results from a fibril with ± 1.0 nm of variability in the repeat spacing, evenly distributed across the interval. Given the clear 1/x dependence in both panels, this figure demonstrates that the 2D FFT method is insensitive to pixel sizes, meaning that as long as features can be resolved experimentally, the D-Period length can be determined without bias from the pixel size of the image or the orientation of the fibril within the image.

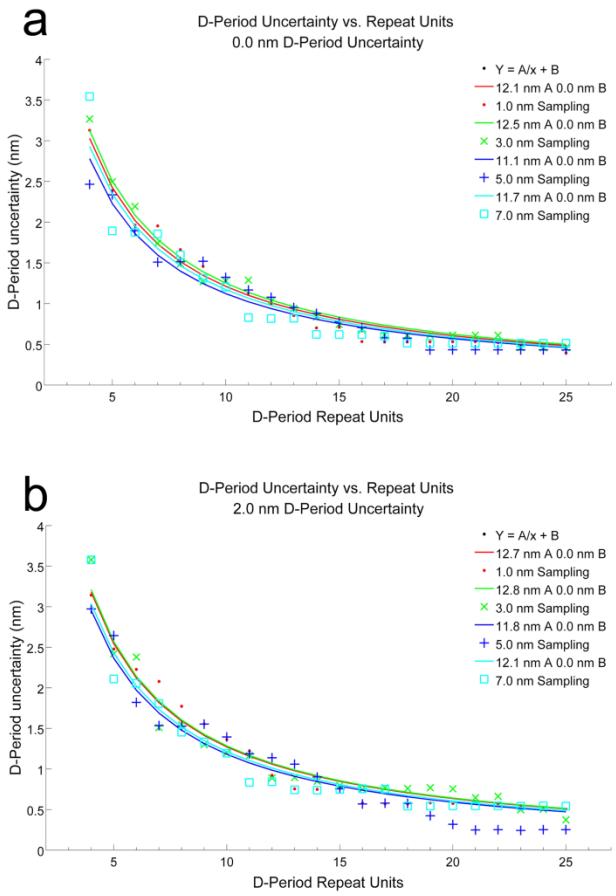
a
D-Period Uncertainty vs. Repeat Units
0.0 nm D-Period Uncertainty
Y = A/x + B
12.1 nm A 0.0 nm B
1.0 nm Sampling
12.5 nm A 0.0 nm B
3.0 nm Sampling
11.1 nm A 0.0 nm B
5.0 nm Sampling
11.7 nm A 0.0 nm B
7.0 nm Sampling
D-Period uncertainty (nm)
D-Period Repeat Units
b
D-Period Uncertainty vs. Repeat Units
2.0 nm D-Period Uncertainty
Y = A/x + B
12.7 nm A 0.0 nm B
1.0 nm Sampling
12.8 nm A 0.0 nm B
3.0 nm Sampling
11.8 nm A 0.0 nm B
5.0 nm Sampling
12.1 nm A 0.0 nm B
7.0 nm Sampling
D-Period uncertainty (nm)
D-Period Repeat Units

SUPPORTING DISCUSSION #2: The nonlinear relationship between AFM scanner error and scan size

AFM scanners can be characterized by the sensitivity which is defined as the ratio of piezo movement to piezo voltage (V). The inherent properties of open loop AFM dictate that the sensitivity varies non-linearly with respect to scan size. In order to test to what extent the nonlinear sensitivity affects the AFM scanner error, we used three calibration standards with pitch sizes of 100 nm, 1 μm and 10 μm. The absolute errors of these calibration standards were examined by SEM to be less than 1.5% (see Supporting Figure S1). The AFM was calibrated using the manufacturer's recommended method, using a 10 μm pitch calibration standard, scanning over the full 80 μm scale of the AFM scanner. After calibration, the percentage errors on the fast and slow scan direction were 2% and 3% respectively, as shown in Supporting Table S2. However, as the scan size decreased, the error increased substantially. Using a 100 nm pitch calibration standard to test the scanner calibration on a 3.5 μm scan, which is the scan size used for acquiring collagen nanomorphologies, the errors on the fast and slow scan direction were 9% and 17% respectively. The Agilent 5500 AFM uses separate piezoelectric elements for X/Y movement and for Z movement. This configuration helps to reduce the cross coupling between different axes, and it also explains the differential responses of piezo-sensitivity on X and Y direction. The effect of nonlinear sensitivity is also shown in Supporting Figure S4. Since the AFM was calibrated over scans of 80 μm size, sensitivity at high voltage ($Sensitivtity_{high\_V}$) was recorded in the calibration file. Therefore AFM Measured Distance always equals voltage times $Sensitivity_{high\_V}$; however the realistic distance on the Standard at small scan sizes equals to voltage times $Sensitivity_{low\_V}$. Comparing the slopes of the linear fittings reveals that $Sensitivity_{low\_V}$ is lower than $Sensitivity_{high\_V}$. This is confirmed after we recalibrated the AFM using 100 nm pitch sized standard over 3.5 μm scale. The X and Y sensitivities decreased from (209.4, 295.5) nm/V to (187.8, 259.1) nm/V. Depending on the piezoelectric material and its configuration in the AFM, the nonlinear relationship between scanner error and scan size could vary and it should be carefully examined. Calibration at the same scale of the

imaging feature size is highly recommended for quantitative analysis.

Supporting Table S2: The Impact of AFM Calibration using the factory recommended 10 x 10 µm standard. The table shows the calculation of scanner errors at different scan size. In this case, the AFM was calibrated using 10 µm x 10 µm calibration standard on 80 µm scale. Due to the nonlinear relationship between scanner error and scan size, the percentage error increased with decreasing scan size. As the scan size decrease from 70 µm to 2 µm, the fast scan direction (X)'s percentage error increased from 2% to 9%; the slow scan direction (Y)'s percentage error increased from 3% to 18%. X and Y direction showed different nonlinear relationship due to the configuration of the Agilent 5500 AFM, which uses separate piezoelectric elements for X, Y and Z movement.

Calibration Standard	Scan Size (µm)	# of Pitches[a]	Fast Scan Direction (X)				Slow Scan Direction (Y)			
			Pitch Size (µm)[b]	Distance on Standard (µm)[c]	Distance by AFM (µm)	% Error	Pitch Size (µm)[b]	Distance on Standard (µm)[c]	Distance by AFM(µm)	% Error
NANOSENSORS-100 nm	2	10	0.1014	1.014	1.109	9.37	0.1009	1.009	1.188	17.74
NANOSENSORS-100 nm	3.5	20	0.1014	2.028	2.214	9.17	0.1009	2.018	2.366	17.24
NANOSENSORS-100 nm	5	40	0.1014	4.056	4.386	8.14	0.1009	4.036	4.612	14.27
NANOSENSORS-100 nm	7	60	0.1014	6.084	6.587	8.27	0.1009	6.054	6.925	14.39
NANOSENSORS-100 nm	10	80	0.1014	8.112	8.600	6.02	0.1009	8.072	9.039	11.98
DI-1 µm[d]	10	8	1.006	8.048	8.689	7.96	1.01	8.080	9.259	14.59
DI-1 µm[d]	20	16	1.006	16.10	17.14	6.46	1.01	16.16	17.99	11.32
DI-1 µm[d]	35	28	1.006	28.17	29.67	5.32	1.01	28.28	30.53	7.96
ASYLUM-10 µm	40	3	10.12	30.36	31.24	2.90	10.15	30.45	31.85	4.60
ASYLUM-10 µm	50	4	10.12	40.48	41.70	3.01	10.15	40.60	42.79	5.39
ASYLUM-10 µm	70	6	10.12	60.72	61.81	1.80	10.15	60.90	62.56	2.73

[a] Number of pitches included in the measurements;

[b] Pitch size measured by SEM;

[c] Distance on Standard = # of Pitches x Pitch Size;

[d] DI is short for Digital Instrument.

Supporting Figure S4: The correlation between AFM measured distance and the distance on the calibration standard (based on SEM results). Panel a represents the correlation on the fast scan (X) direction and panel b represents that of slow scan (Y) direction. Blue diamonds are measured from 2 – 10 µm scan sizes using NANOSENSORS's 100 nm x 100 nm standard; red squares are measured from 10-35 µm scan sizes using Digital Instrument's 1 µm x 1 µm standard; green triangles are measured from 40-70 µm scan sizes using Asylum Research's 10 µm x 10 µm standard. The equations are linear fitting of these three individual scales, the linear fitting of the blue and green dots is plotted for visual comparison.

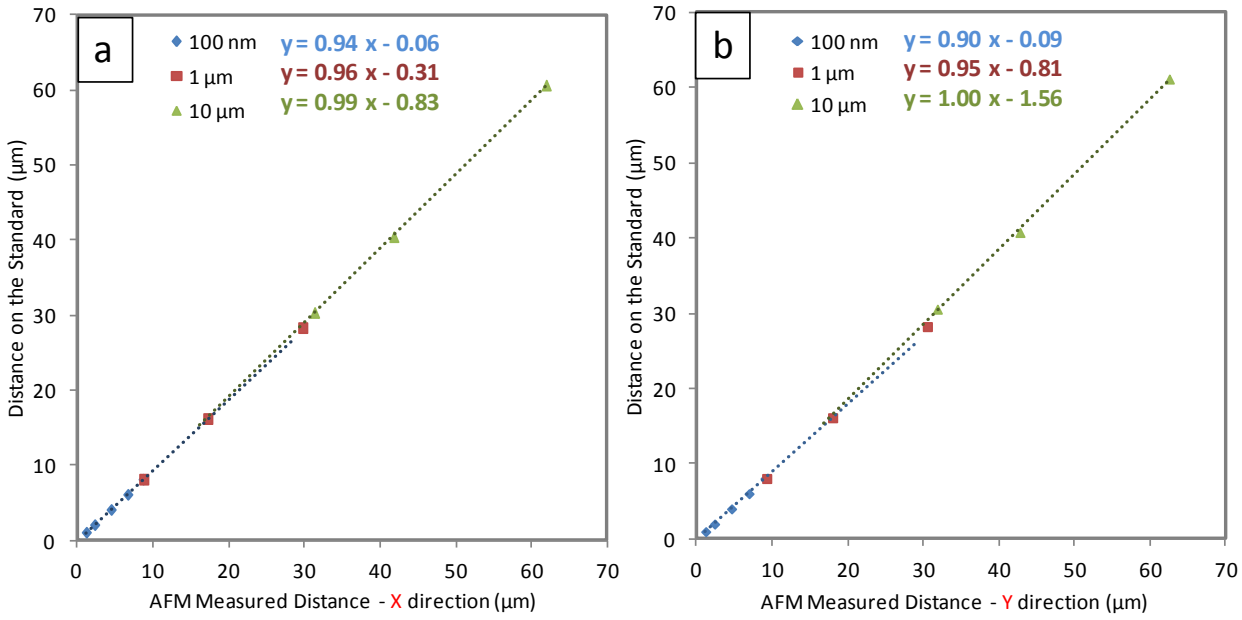

Supporting Figure S5: Influence of Thermal Drift on the Measured D-Periodic Spacing. This figure shows how the measured D-Period changes in up scans versus down scans as the same 3.5 µm x 3.5 µm location is scanned over time. Scanning was at 2 Hz with 512 lines, so each scan took 256 seconds (approximately 4.3 minutes per scan or 73 minutes total). Over this time scale, the effect of thermal drift on the measured D-spacing of 3 fibrils was 1.2 ± 0.5 nm. The discrepancy between up and down scans could be explained by the fact that the piezo scanner exhibits more sensitivity at the end than the beginning of a scan, causing the up and down scans to behave differently and display hysteresis between the two scan directions.[2]

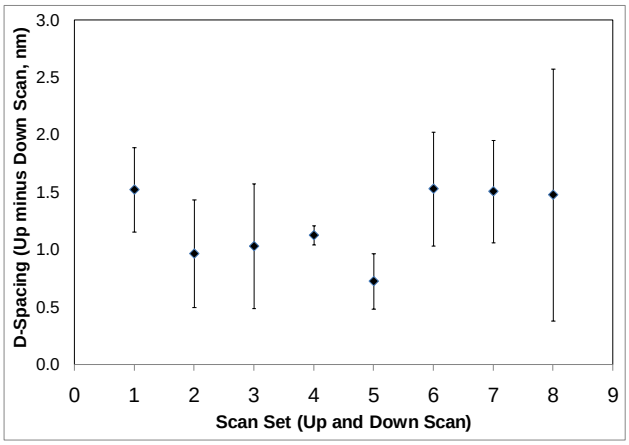

Supporting Figure S6: D-Periodic Spacing as a Function of Fibril Angle. Angle is measured with 0 degrees along the fast scan axis and goes from -90 to 90 degrees. The data is represented on a Cartesian plot (b) as well as a polar plot (c). This figure demonstrates that the fibril angle does not introduce systematic errors in the D-spacing distribution. This suggests that magnitudes of such systematic errors, for example originating from thermal drift or asymmetry in the x-y piezos, are small enough that they do not impact the D-spacing measurement.

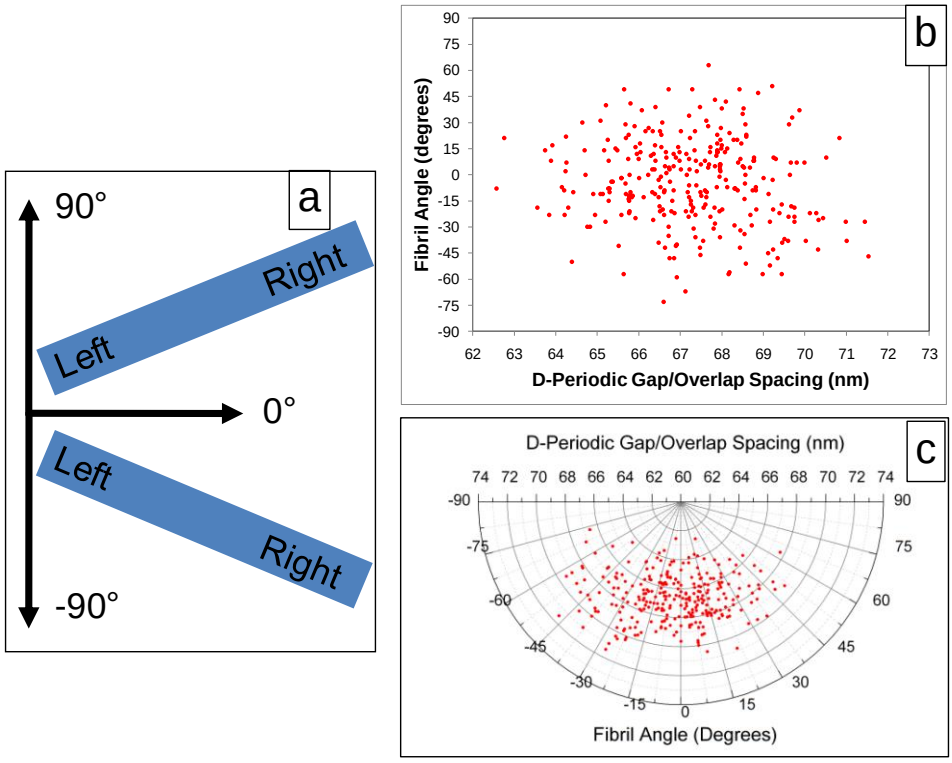

SUPPORTING DISCUSSION #3: Investigation of historical SAXS data

To investigate other methods that have been used to analyze Type I Collagen morphology, historical Small Angle X-Ray Scatter (SAXS) data from fresh, non-mineralized, turkey tendon samples were analyzed (Figure 5).[3] Multiple D-period harmonics are present in this curve. This image was analyzed to determine if inhomogeneity in D-period spacing is sufficient to explain the observed peak widths from SAXS analyses of collagen. A modified Bertaut-Warren-Averbach (BWA) technique, as outlined by Drits[4] was used to determine what portion of the peak widths can be ascribed to inhomogeneity in D-Period spacing. This analysis will demonstrate if the distribution of D-Period spacings measured by AFM is consistent with the observed widths of X-Ray peaks. Initially, the data was digitized and scaled from the published image to provide a working data set. The resulting data was linearly interpolated to provide even scaling along the x-axis. The background intensity (areas that were not clearly peaks) was fit to the form: $Y = Ax^{-B} + C$ where A = 1.1, B = -3.2, C = 10.9. This fitted form is simply an approximation to the background scattering intensity from the sample. Since the observed intensity is defined by BWA as the product of the background intensity and scattering peaks, the observed spectrum was normalized against the fitted background. For future studies, a blank spectrum is a more appropriate background to use. The results are shown in Figure 5 in the main body of the paper.

In order to determine the uncertainty in the D-Period spacing, a variant of the BWA technique was applied to extract the underlying distribution of D-Periodic spacings from the scattering peaks. Drits initially describes the intensity from a sample as the product of the Lorentz and polarization factors, the structure factors, and interference function (Drits, Equation 1). The interference can then be determined by dividing the scattering by these background components (Drits, Equation 2). Background correction was accomplished by dividing the scattering intensity by the fitted background. Each peak was fit to a Gaussian in order to identify the peak center of each scattering harmonic in reciprocal space. The reciprocal values of the spacing reported on the x-axis were computed and multiplied by the appropriate harmonic to determine the real values of the D-Periodic spacing. Baseline could not be adequately

separated from peak intensity at low x values for the first harmonic. The Gaussian fit to the first harmonic may not be accurate and appears to be biased to higher value in reciprocal space (shorter D-Period spacing). Because of this apparent bias, the first harmonic is excluded from the average calculation. The average D-Periodic spacing (harmonics 2 through 6) was determined to be 64.2 ± 0.6 nm. The extracted D-Period spacings are shown in Supporting Figure S7.

Supporting Figure S7: SAXS D-Period Spacing. The calculated D-Period spacing from each harmonic in Figure 5 is shown above. The first harmonic is not included in the average because a lack of baseline on both sides of the peak leads to a bias in the Gaussian Fit. The average D-Period spacing is 64.2 ± 0.6 nm.

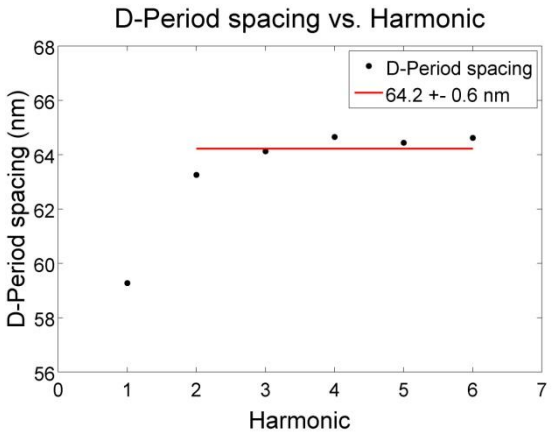

Drits states that the scattering intensity for a sample with a known D-Period spacing can be described as a Fourier series (Drits, Equation 13), the coefficients of which can be determined by an inverse Fourier transform (Drits, Equation 14). Since these coefficients can be calculated analytically, they provide a useful way to investigate the scattering curves. In the case that the D-Period spacing is not uniform, and there is a distribution of spacings around a given mean, the scattering intensity can still be fully described by a Fourier series (Drits, Equation 20). This new series can also be inversely transformed to generate a different set of Fourier coefficients (Drits, Equation 21), which can be simplified, since the scattering peaks are symmetric, to a sum of cosine terms (Drits, Equation 23).

Assuming an independent and identical distribution of D-Period spacings, which approximates distributions observed by AFM, the reduced Fourier coefficients can be written as the product of the coefficients from a perfect sample and a different Gaussian modifying term, the parameters of which describe the distribution of spacings (Drits, Equation 26), which is both separable and linear (Drits, Equation 27). This means that one can take a set of observed scattering peaks, Fourier transform them and fully separate the pure scattering components from broadening because of variation in D-Period spacings.

This method was applied to the baseline corrected turkey tendon data in the following way. Each peak was separated onto an interval spanning the average peak separation centered on the peak. The peak center used is the center from the Gaussian fits used to determine the average D-Period spacing. This interval was scaled by the average peak separation so that the final interval was symmetric ranging from -½ to ½ with a peak centered at 0. The Fourier transform of the scattering peak over this symmetric interval was then computed in order to extract the components. Since the coefficients are required to be strictly positive and the sine terms sum to 0, the amplitude of the overall transform was used for the next calculations. Transforming the raw data or fitted Gaussian yield identical results. The transform of harmonic three is shown as an example in Supporting Figure S8.

Supporting Figure S8: Example BWA Transform. This figure shows an example of the transforms used to calculate the distribution of D-Period spacings. In the upper panel the blue dots are the baseline corrected scattering intensity. The red line is a Gaussian fit to this peak. The peak has been centered over a scaled interval spanning the average reciprocal D-Period Spacing. Below is the Fourier transform of the above data. The dots are transforms of the raw data, and the solid lines are the transforms of the Gaussian fit. In blue are the cosine components, red are the average components, green is the amplitude of the transform, and teal the absolute value of just the cosine component.

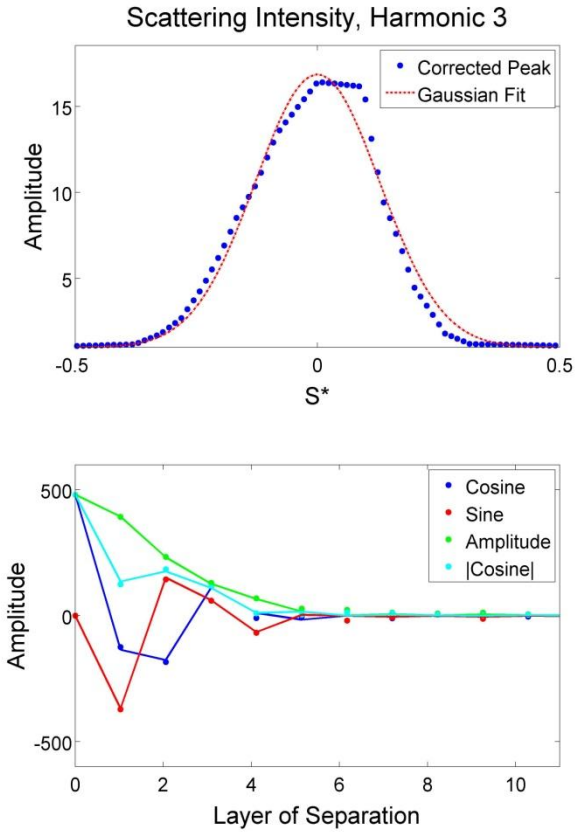

Following Drits' method, a plot of the Fourier coefficients (A_n) vs. the square of the harmonic (l^2) was constructed. The slope of the line contains the information about the distribution of D-Period spacings:

$$m = \frac{-2\pi^2 n \overline{\sigma_1^2}}{d^2(001)}$$

$$\overline{\sigma_1} = \sqrt{-\frac{m d^2(001)}{2\pi^2 n}}$$

where m is the slope of the line, n is the number of the coefficient, $\overline{\sigma_1}$ is the standard deviation of the distribution of D-Period spacings around $d(001)$, the reciprocal of the D-Period spacing (Supporting Figure S9).

For this particular data set, the first, third, fifth and sixth harmonics were used to calculate the distribution of D-Period spacings. Harmonic one cannot be included, in this case, because each peak is required to be centered at 0. Fratzl notes significant dampening in amplitude of harmonics two and four, which he suggests arises from partial hydration of the fibril leading to reduced contrast.[2] Since this method is dependent on the relative amplitudes of the different scattering harmonics, these two harmonics must be excluded. The calculated standard deviation of the D-Period spacing is 2.1 nm. The extracted D-Period spacing is shown below in Supporting Figure S10.

Supporting Figure S9: Fit of ln(A_n) vs. l^2. This figure plots the natural log of the Fourier coefficients (separated by n layers) of each peak against the square of the harmonic. The slope of each line is calculated in order to determine the distribution of D-Period spacings.

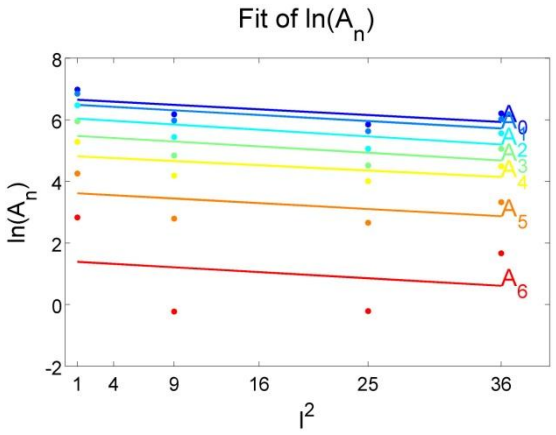

Supporting Figure S10: SAXS Calculated Standard Deviation of D-Period Distribution. This Figure shows the calculated D-Period standard deviations calculated from Figure 5. The average D-Period standard deviation is 2.1 nm.

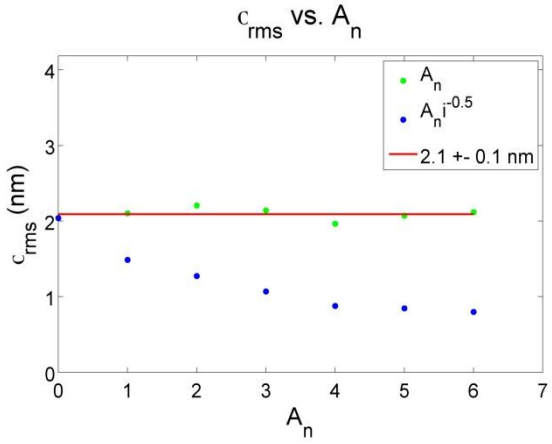

This analysis had two main findings. First, inhomogeneity in the D-Period spacing is sufficient to explain the observed peak width in X-Ray data. Second, the distribution width determined from the X-Ray analysis was comparable to the distribution width observed using the 2D-FFT technique on individual fibrils. One significant advantage of the 2D-FFT technique is that the fundamental resolution limit is sufficiently small to directly observe the shape of the sample distribution. By definition, the modified BWA technique cannot observe the sample distribution shape because only one distribution is defined in the algebra, and the ability to fit the transformed data is insufficient to discriminate between different functional forms for an underlying distribution.

(1) Arfken, G. B.; Weber, H. J. In *Mathematical Methods for Physicists;* Elsevier Academic Press: Burlington, MA, **2005**; pp 2000.

(2) Lapshin, R. V., Analytical model for the approximation of hysteresis loop and its application to the scanning tunneling microscope. *Rev. Sci. Instrum.* **1995,** *66* , 4718-4730.

(3) Fratzl, P.; Fratzl-Zelman, N.; Klaushofer, K. Collagen Packing and Mineralization. an x-Ray Scattering Investigation of Turkey Leg Tendon. *Biophys. J.* **1993***, 64*, 260-266.

(4) Drits, V. A.; Eberl, D. D.; Srodon, J. XRD Measurement of Mean Thickness, Thickness Distribution and Strain for Illite and Illite-Smectite Crystallites by the Bertaut-Warren-Averbach Technique. *Clays Clay Miner.* **1998***, 46*, 38-50.